Magnetic phase transition in two-dimensional *XY* random spin system: stage-2 $Cu_cCo_{1-c}Cl_2$ graphite intercalation compounds

1999 J. Phys.: Condens. Matter 11 521

(http://iopscience.iop.org/0953-8984/11/2/016)

J. Phys.: Condens. Matter **11** (1999) 521–541. Printed in the UK PII: S0953-8984(99)92325-1

Magnetic phase transition in two-dimensional XY random spin system: stage-2 $Cu_cCo_{1-c}Cl_2$ graphite intercalation compounds

Itsuko S Suzuki and Masatsugu Suzuki

Department of Physics, State University of New York at Binghamton, Binghamton, NY 13902-6016, USA

Received 9 March 1998, in final form 14 September 1998

Abstract. The magnetic phase transition of a two-dimensional (2D) random spin system with competing exchange interactions, stage-2 $Cu_cCo_{1-c}Cl_2$ GICs, has been studied using SQUID AC magnetic susceptibility and SQUID DC magnetization. The magnetic phase diagram of critical temperature versus Cu concentration is determined. For $0 \leqslant c \leqslant 0.3$ the system undergoes two phase transitions at T_{cu} and T_{cl} ($T_{cu} > T_{cl}$). Below T_{cu} a 2D ferromagnetic order is established in each intercalate layer. Below T_{cl} there appears a 3D antiferromagnetic phase with the 2D ferromagnetic layers being antiferromagnetically coupled along the c-axis. For $0.4 \leqslant c \leqslant 0.9$ the system undergoes a phase transition at T_c ($= T_{cl}$) and a reentrant spin glass transition at T_{RSG} ($< T_{cl}$). For $0.9 < c \leqslant 0.93$ the system undergoes a spin glass transition at T_{SG} from the paramagnetic phase to the spin glass phase. No phase transition is observed for $c = 1$ at least above 0.3 K because of the fully frustrated nature of the 2D antiferromagnet on the triangular lattice. The enhancement of T_c in the intermediate concentration and the positive sign of the Curie–Weiss temperature for $c < 0.83$ indicates that the intraplanar interaction between Cu^{2+} and Co^{2+} spins is ferromagnetic. The nature of the ferromagnetic phase, reentrant spin glass phase and spin glass phase is examined from the frequency dependence of absorption χ''.

1. Introduction

Recently the magnetic properties of magnetic random-mixture graphite intercalation compounds (RMGICs) have received considerable attention. These RMGICs provide model systems for studying two-dimensional (2D) random spin systems with various kinds of spin frustration effect such as competing ferromagnetic (FM) and antiferromagnetic (AF) interactions, and competing spin anisotropies between Ising, XY and Heisenberg symmetries. Stage-2 $Cu_cCo_{1-c}Cl_2$ GICs, which are typical examples of RMGICs, magnetically behave like a 2D XY random spin system with competing FM and AF short-ranged exchange interactions [1]. Cu^{2+} and Co^{2+} ions are randomly distributed on the triangular lattice sites. The intraplanar exchange interaction between Co^{2+} ions, J(Co–Co), is ferromagnetic, while that between Cu^{2+} ions, J(Cu–Cu), is antiferromagnetic: J(Co–Co) $= 7.75$ K and J(Cu–Cu) $= -33.63$ K. The sign of the Curie–Weiss temperature changes from positive to negative with increasing concentration around $c = 0.8$ to 0.85. This result indicates that the intraplanar exchange interaction J(Cu–Co) between Cu^{2+} and Co^{2+} spins is ferromagnetic and depends on the Cu concentration c : J(Cu–Co) $= 57.94c^3$ [K]. Note that J(Cu–Co) is 7.75 K at $c = 0.51$ which is comparable to J(Co–Co) and is 33.63 K at $c = 0.83$ which is comparable to $|J$(Cu–Cu)$|$.

0953-8984/99/020521+21$19.50

This concentration dependence of J(Cu–Co) can be explained as follows. The non-Jahn–Teller Co^{2+} and the Jahn–Teller Cu^{2+} ions are randomly distributed on the triangular lattice. For $c \approx 0$, Cu^{2+} ions may be located on a triangular lattice with sides $a = 3.55$ Å formed by Co^{2+} ions in the $CoCl_2$ layer, while for $c \approx 1$, Co^{2+} ions may be located on an isosceles triangular lattice with one short side ($a_1 = 3.30$ Å) and two longer sides ($a_2 = 3.72$ Å) formed by Cu^{2+} ions in the $CuCl_2$ layer. Thus a possible change in the average distance between Cu^{2+} and Co^{2+} ions with Cu concentration gives rise to a change in J(Cu–Co) with Cu concentration.

In this paper we study the magnetic phase transitions of stage-2 $Cu_cCo_{1-c}Cl_2$ GICs ($0 \leqslant c \leqslant 1$) using SQUID DC magnetization and SQUID AC magnetic susceptibility with various frequencies. The magnetic phase diagram of these compounds is rather complicated because of spin frustration effects arising from both (i) competing interactions and (ii) the frustrated nature of the antiferromagnet on the triangular lattice. A long range ordered phase below ≈9 K observed for $c = 0.1$, 0.2 and 0.3 is essentially the same as that for $c = 0$. For $0.4 \leqslant c \leqslant 0.9$ the system enters into a reentrant spin glass (RSG) phase around 3–4 K from the high temperature FM phase observed below ≈9 K. The transition from the paramagnetic (PM) phase to the spin glass (SG) phase is observed around 7 K for $c = 0.93$. The nature of the RSG phase and SG phase is discussed considering the frequency (f) and temperature (T) dependence of the absorption χ''. The origin of RSG and SG phases is discussed in association with relevant theories.

The format of this paper is as follows. The related background is presented in section 2. The experimental procedure and result are given in sections 3 and 4, respectively. A discussion and conclusion are given in sections 5 and 6, respectively.

2. Magnetic properties of stage-2 $CuCl_2$ and $CoCl_2$ GICs

Stage-2 $CuCl_2$ GIC magnetically behaves like a 2D Heisenberg antiferromagnet (spin $S = 1/2$) with small XY anisotropy on an isosceles triangular lattice with one short side ($a_1 = 3.30$ Å) and two longer sides ($a_2 = 3.72$ Å) [2]. In spite of this lattice distortion due mainly to the Jahn–Teller effect, the exchange interaction between nearest neighbour Cu^{2+} spins along the $\boldsymbol{a}_1$-axis (J_1) is the same as that between nearest neighbour Cu^{2+} spins along the $\boldsymbol{a}_2$-axis (J_2): ($J_1 = J_2 = \langle J \rangle = -33.6$ K). The susceptibility of stage-2 $CuCl_2$ GIC exhibits a broad peak of magnitude χ_{max} ($= 3.014 \times 10^{-3}$ emu/mol Cu) at the temperature T_{max} ($= 62$ K) [2]. These values of χ_{max} and T_{max} are in good agreement with those predicted from a theory on the susceptibility of a 2D Heisenberg antiferromagnet. No magnetic phase transition is observed either by DC magnetic susceptibility down to 1.5 K or by magnetic neutron scattering down to 0.3 K [2], partly because of the fully frustrated nature of the antiferromagnet on the triangular lattice.

Stage-2 $CoCl_2$ GIC magnetically behaves like a 2D Heisenberg ferromagnet (fictitious spin $S = 1/2$) with large XY anisotropy [3, 4]. The Co^{2+} ions form a triangular lattice with side $a = 3.55$ Å. The spin Hamiltonian for Co^{2+} ions is described by the intraplanar exchange interaction ($J = 7.75$ K), the anisotropic exchange interaction J_A ($J_A/J = 0.48$) showing XY anisotropy, and the antiferromagnetic interplanar exchange interaction J'. The antiferromagnetic interplanar exchange interaction is very weak compared to the intraplanar exchange interaction: $|J'|/J = 8 \times 10^{-4}$. The T-dependence of absorption χ'' clearly indicates that this compound undergoes at least two magnetic phase transitions at $T_{cu} = 8.9$ K and $T_{cl} = 6.9$–7.1 K [5]. Above T_{cu}, the system is in the PM phase. In the intermediate phase between T_{cl} and T_{cu}, a 2D spin long range order is established. A 3D AF phase appears below T_{cl} where the 2D ferromagnetic layers are antiferromagnetically stacked along the c-axis [6].

3. Experiment

The samples used in the present experiments were the same as those reported before [1]. Stage-2 $Cu_cCo_{1-c}Cl_2$ GIC samples with $c \geqslant 0.4$ were prepared by intercalation of single crystal $Cu_cCo_{1-c}Cl_2$ into highly oriented pyrolytic graphite (HOPG): the mixture of HOPG and $Cu_cCo_{1-c}Cl_2$ was heated at 450 °C for 14 days in Pyrex glass sealed in vacuum. The samples with $0 \leqslant c \leqslant 0.3$ were prepared by intercalation of $Cu_cCo_{1-c}Cl_2$ into single crystals of kish graphite (SCKG): the mixture of SCKG and $Cu_cCo_{1-c}Cl_2$ was heated at 520 °C for 20 days in chlorine gas atmosphere at a pressure of 740 Torr. The Cu concentration of these compounds was determined from electron microprobe measurement with a scanning electron microscope (model Hitachi S-450). The c-axis repeat distance d, Curie–Weiss temperature Θ, the effective magnetic moment P_{eff} and the value n of these compounds are listed in table 1, where the stoichiometry is described by $C_nCu_cCo_{1-c}Cl_2$. It is predicted from the molecular field theory [1] that P_{eff} changes with Cu concentration c as $P_{eff}(c) = \{c[P_{eff}(\mathrm{Cu})]^2 + (1-c)[P_{eff}(\mathrm{Co})]^2\}^{1/2}$ where $P_{eff}(\mathrm{Cu})$ ($= 2.26\ \mu_B$) and $P_{eff}(\mathrm{Co})$ ($= 5.54\ \mu_B$) are the effective magnetic moments for stage-2 $CuCl_2$ GIC and stage-2 $CoCl_2$ GIC. The Cu concentration determined from P_{eff} is in good agreement with that from electron microprobe measurement, suggesting that Cu^{2+} and Co^{2+} are randomly distributed in the intercalate layers.

Table 1. Sample characterization of stage-2 $Cu_cCo_{1-c}Cl_2$ GICs, where Θ is the Curie–Weiss temperature, P_{eff} is the effective magnetic moment and d is the c-axis repeat distance. The stoichiometry is described by $C_nCu_cCo_{1-c}Cl_2$.

c	Θ (K)	P_{eff} (μ_B/av. atom)	d (Å)	n
1	−100.9	2.26	12.81 ± 0.05	11.19
0.93	-43.76 ± 0.55	2.55	12.80 ± 0.05	11.42
0.9				15.47
0.88				14.11
0.8	2.52 ± 0.22	2.98	12.83 ± 0.05	11.04
0.7	8.31 ± 0.31	3.47	12.83 ± 0.24	11.54
0.5	14.48 ± 1.35	3.69	12.83 ± 0.05	13.35
0.4	19.19 ± 0.28	4.02		13.50
0.3				11.04
0.2	19.07 ± 0.27	6.18	12.84 ± 0.15	15.78
0.1	25.29 ± 0.29	6.01	12.79 ± 0.10	10.96
0	23.2	5.54	12.79 ± 0.01	9.87

The SQUID DC magnetization and AC magnetic susceptibility of stage-2 $Cu_cCo_{1-c}Cl_2$ GICs with $c = 0$, 0.1, 0.2, 0.3, 0.4, 0.5, 0.7, 0.8, 0.88, 0.9 and 0.93 were measured using a SQUID magnetometer (Quantum Design MPMS XL-5) with ultra-low field capability. The SQUID DC magnetization measurement was carried out as follows. First the remanent magnetic field was reduced to zero (actually ∼3 mOe) at 298 K. Then the sample was cooled to 1.9 K in the zero magnetic field. Then the magnetic field of 1 Oe was applied along any direction perpendicular to the c-axis. The zero field cooled magnetization (M_{ZFC}) was measured with increasing T from 1.9 to 20 K and field cooled magnetization (M_{FC}) was measured with decreasing T from 20 to 1.9 K. The SQUID AC magnetic susceptibility measurement was carried out as follows. First the sample was cooled in zero magnetic field. Then the SQUID AC magnetic susceptibility along the c-plane was measured with increasing T from 1.9 to

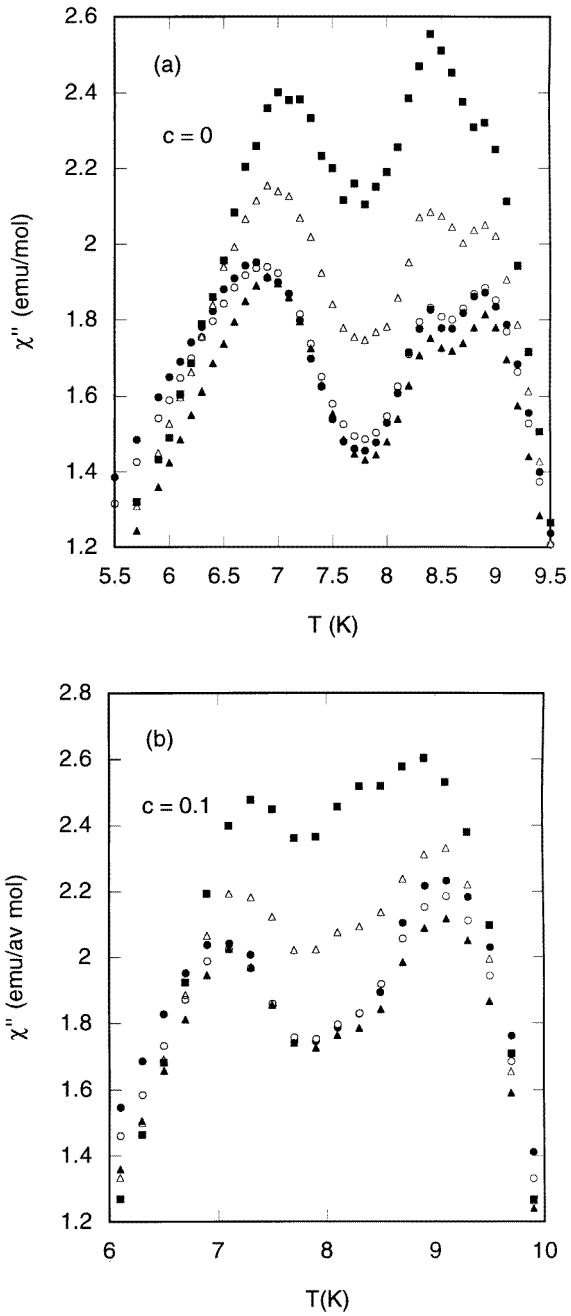

Figure 1. χ'' against T for (a) $c = 0$, (b) $c = 0.1$, (c) $c = 0.2$ and (d) $c = 0.3$. $f = 0.1$ (●), 1 (○), 10 (▲), 100 (△) and 1000 Hz (■). $H = 0$. $h = 50$ mOe. $h \perp c$. The T-dependence of χ' with $f = 0.1$ Hz for $c = 0.3$ is shown in the inset of (d).

15 K with and without an external magnetic field. Both an ac magnetic field with amplitude h (= 50 mOe) and frequency f (= 0.007–1000 Hz) and an external dc magnetic field H (= 0–1 kOe) were applied along the c-plane (any direction perpendicular to the c-axis).

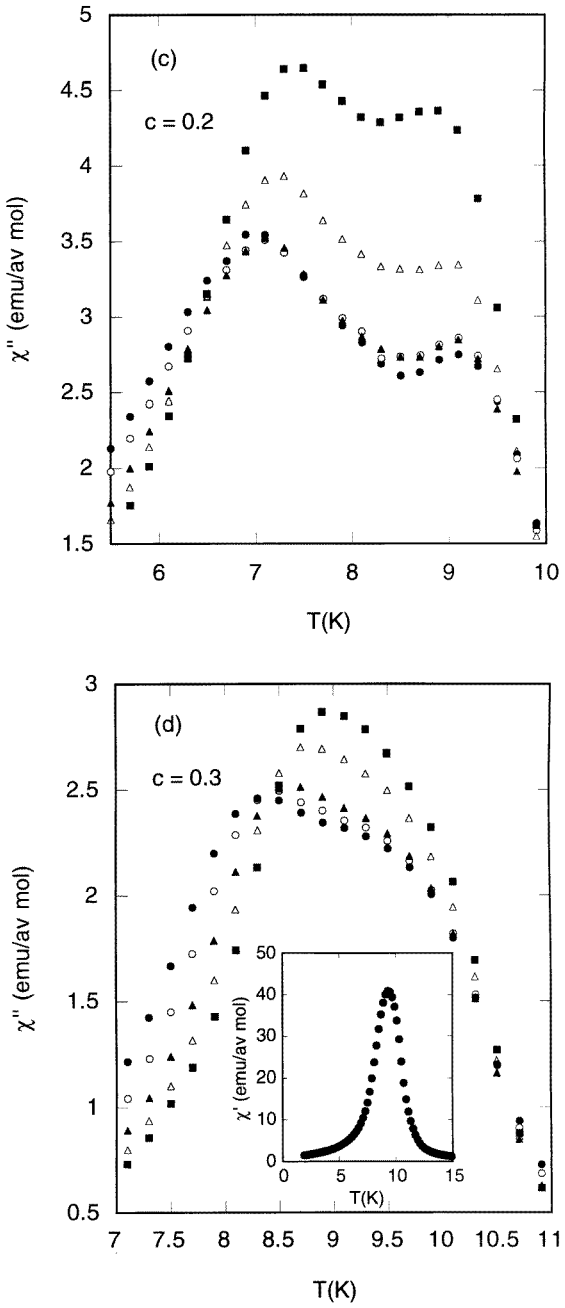

Figure 1. (Continued)

4. Result

4.1. FM phase: $0 \leqslant c \leqslant 0.3$

Figure 1 shows the T-dependence of χ'' for (a) $c = 0$, (b) $c = 0.1$, (c) $c = 0.2$ and (d) $c = 0.3$ for various f. For $c = 0$ χ'' shows three peaks at T_{cu}, T_{p2} and T_{cl} which are independent of f:

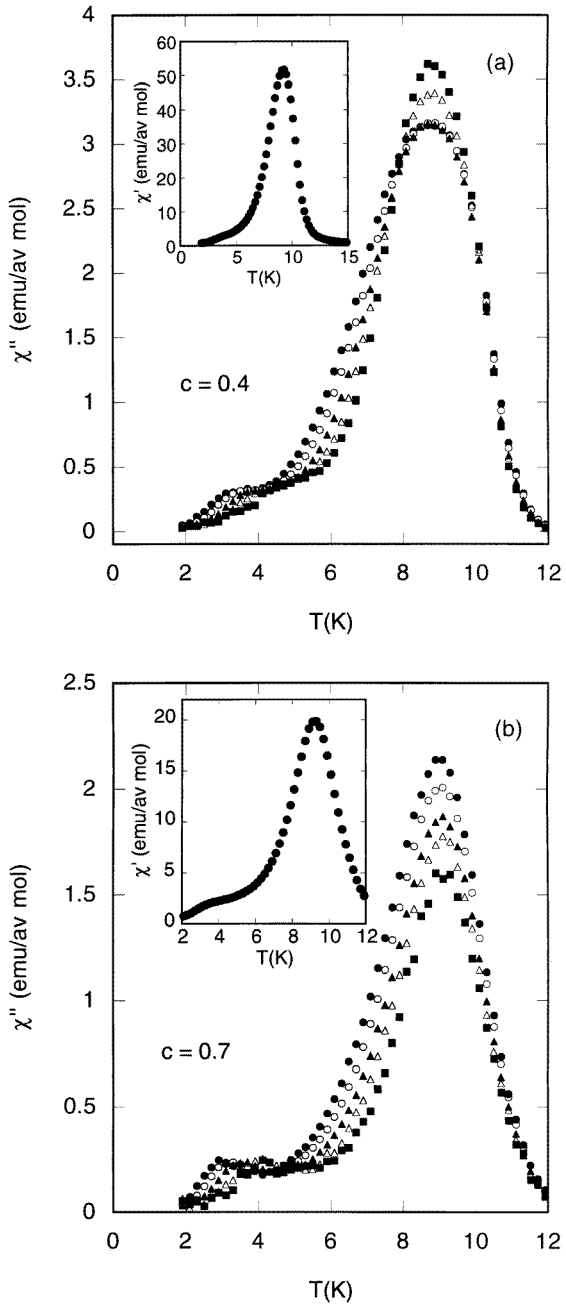

Figure 2. χ'' against T for (a) $c = 0.4$, (b) $c = 0.7$ and (c) $c = 0.8$. $f = 0.1$ (●), 1 (○), 10 (▲), 100 (△) and 1000 Hz (■). $H = 0$. $h = 50$ mOe. $h \perp c$. The T-dependence of χ' with $f = 0.1$ Hz for $c = 0.4$ and 0.7 is shown in the insets of (a) and (b), respectively.

$T_{cu} = 8.9$ K, $T_{p2} = 8.4$ K and $T_{cl} = 6.9$ K [5]. The dispersion χ' at $c = 0$ has a single peak at $T_{p2} = 8.4$ K independent of f [5]. The 2D FM order develops in the $CoCl_2$ intercalate layer below T_{cu}, and 3D AF order is established below T_{cl} through an AF interplanar interaction.

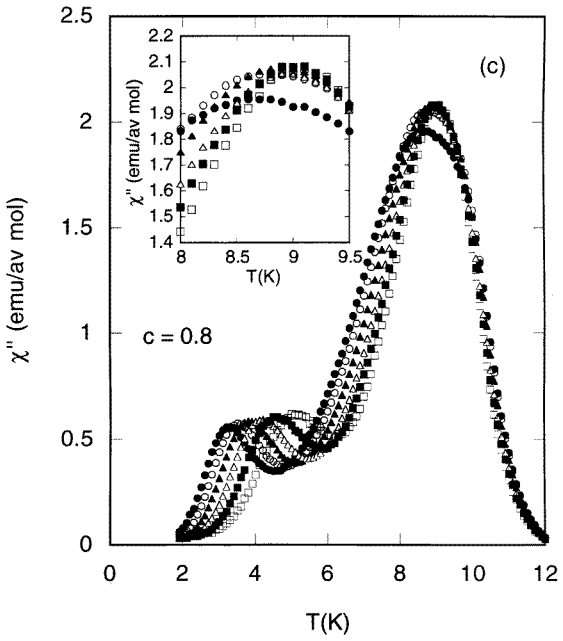

Figure 2. (Continued)

Hereafter for convenience the ordered phase below T_{cu} is denoted as a FM phase because the spins in each intercalate layer are ferromagnetically ordered.

For $c = 0.1$ χ'' also has three peaks at T_{cu}, T_{p2} and T_{cl}. The value of T_{p2} is around 8.3 K at $f = 1$ kHz. The value of T_{cu} slightly decreases from 9.1 K at $f = 0.1$ Hz to 8.9 K at 1 kHz, while the value of T_{cl} increases from 7.0 K at $f = 0.1$ Hz to 7.3 K at 1 kHz. The dispersion χ' has a single peak around 8.4 K independent of f.

For $c = 0.2$ χ'' has two peaks at T_{cl} and T_{cu}. The value of T_{cu} decreases from 9.1 K at $f = 0.1$ Hz to 8.85 K at $f = 1$ kHz, while the value of T_{cl} increases from 7.0 K at $f = 0.1$ Hz to 7.4 K at 1 kHz. The dispersion χ' has a single peak at 8.5 K independent of f. The magnetization M_{ZFC} increases with increasing T, shows a broad peak at $T_0 = 8.3$ K and decreases with further increasing T. The magnetization M_{FC} rapidly increases with decreasing T around 9 K and saturates below 8 K. The deviation of M_{FC} from M_{ZFC} appears below $T_f = 10.7$ K, showing an irreversible effect of magnetization.

For $c = 0.3$ χ'' has a shoulder at T_{cu} (= 9.5 K) independent of f and a peak at T_{cl} which increases from 8.4 K at $f = 0.1$ Hz to 9.0 K at 1 kHz. The dispersion χ' has a single peak at 9.4 K independent of f (see the inset of figure 1(d)). The appearance of a shoulder indicates that the nature of the 2D FM order may change by a partial replacement of Co^{2+} ions by Cu^{2+} ions. The probability P(Cu–Co) of finding Cu–Co bonds is comparable to P(Co–Co) for $c = 0.3$, where $P(\text{Co–Co}) = (1-c)^2$ and $P(\text{Cu–Co}) = 2c(1-c)$ [1].

4.2. RSG phase: 0.4 ⩽ c ⩽ 0.9

Figure 2 shows the T-dependence of χ'' for (a) $c = 0.4$, (b) $c = 0.7$ and (c) $c = 0.8$. For $c = 0.4$ χ'' has a peak at T_c (= 8.7–8.9 K) almost independent of f and a broad peak at a temperature T_{RSG} which increases from 3.1 K at $f = 0.1$ Hz to 4.1 K for 1 kHz. The

transition at T_{RSG} is one from the FM phase to the RSG phase. The dispersion χ' has a single peak at 9.2–9.3 K independent of f. Since the critical temperature T_c is lower than the peak temperature of χ', T_c is considered to coincide with T_{cl}.

For $c = 0.7$ χ'' has a peak at T_c which slightly increases from 9.0 K at $f = 0.1$ Hz to 9.15 K at 1 kHz and a broad peak at T_{RSG} which increases from 2.9 K at $f = 0.1$ Hz to 4.1 K for 1 kHz. The dispersion χ' has a single peak at 9.2–9.4 K. Similar behaviours of χ' and χ'' are also observed for $c = 0.5$.

For $c = 0.8$ χ'' has two peaks at T_{RSG} and T_c. The peak at T_{RSG} shifts to the high temperature side with increasing f: 3.20 K at $f = 0.007$ Hz and 5.12 K at 1 kHz. The peak at T_c slightly shifts to the high temperature side with increasing f: 8.7 K at $f = 0.01$ Hz and 9.1 K at 1 kHz [7]. The dispersion χ' has a single peak and a shoulder [7]. The peak shifts slightly from 9.20 to 9.30 K with increasing f from 0.01 Hz to 1 kHz, while the shoulder shifts greatly from 3 to 6 K. The peak height is strongly dependent on f, varying in height by a factor of two. The magnetization M_{ZFC} has a shoulder around 3.5 K and a peak at $T_0 = 9.0$ K [7]. The deviation of M_{ZFC} from M_{FC} appears below $T_f = 12.5$ K, implying the irreversible effect of magnetization occurring below this temperature. The magnetization M_{FC} drastically increases with decreasing T below $\approx$10 K, suggesting that the 2D FM order is established in the intercalate layers.

4.3. SG phase: $c = 0.93$

Figures 3(a) and (b) show the T-dependence of χ' and χ'' for $c = 0.93$ with various f, respectively. The dispersion χ' has a single peak, shifting to the higher temperature side with increasing f: 7.42 K at $f = 0.1$ Hz and 8.0 K at 1 kHz. The peak height greatly decreases with increasing f. The absorption χ'' also has a single peak at T_{SG}, shifting to the higher temperature side with increasing f: 6.3 K at $f = 0.1$ Hz, 6.57 K at 1 Hz, 6.81 K at 10 Hz, 7.2 K at 100 Hz and 7.4 K at 1 kHz, while the peak height does not change with f at all in contrast to that of χ'. The inset of figure 3(a) shows the T-dependence of M_{FC} and M_{ZFC} for $c = 0.93$, where $H = 10$ Oe. The magnetization M_{ZFC} has a peak at $T_0 = 6.3$ K. The deviation of M_{ZFC} from M_{FC} appears below $T_f = 8.5$ K. Note that the magnetic susceptibility defined by M_{FC}/H is much smaller than that for $c = 0.8$ because of the drastic increase in the probability P(Cu–Cu).

4.4. Field dependence of χ''

Figure 4 shows the T-dependence of χ'' for (a) $c = 0.2$, (b) $c = 0.8$ and (c) $c = 0.93$ in the presence of H along the c-plane, respectively, where $f = 100$ Hz and $h = 50$ mOe. For $c = 0.2$ the peak of χ'' at T_{cu} disappears at $H = 5$ Oe, while the peak of χ'' at T_{cl} shifts to the lower temperature side with the peak height drastically decreasing as H increases. This result indicates an AF character of the ordered phase below T_{cl}.

For $c = 0.8$ the peak temperature of χ'', T_{RSG}, decreases as H increases up to 50 Oe (see the inset of figure 4(b)). The peak height drastically decreases with increasing H and reduces to zero above 100 Oe. The data of T_{RSG} against H are well fitted to the form described by

$$H = H_0 \left(1 - \frac{T_{RSG}(H)}{T_{RSG}(H=0)}\right)^a \tag{1}$$

with $H_0 = 581$ Oe, $T_{RSG}(H = 0) = 4.62 \pm 0.08$ K and $a = 1.26 \pm 0.02$. This exponent a is smaller than that ($a = 1.50$) predicted by de Almeida and Thouless (AT) [8] for the field dependence of freezing temperature at the transition between the PM phase and the SG phase.

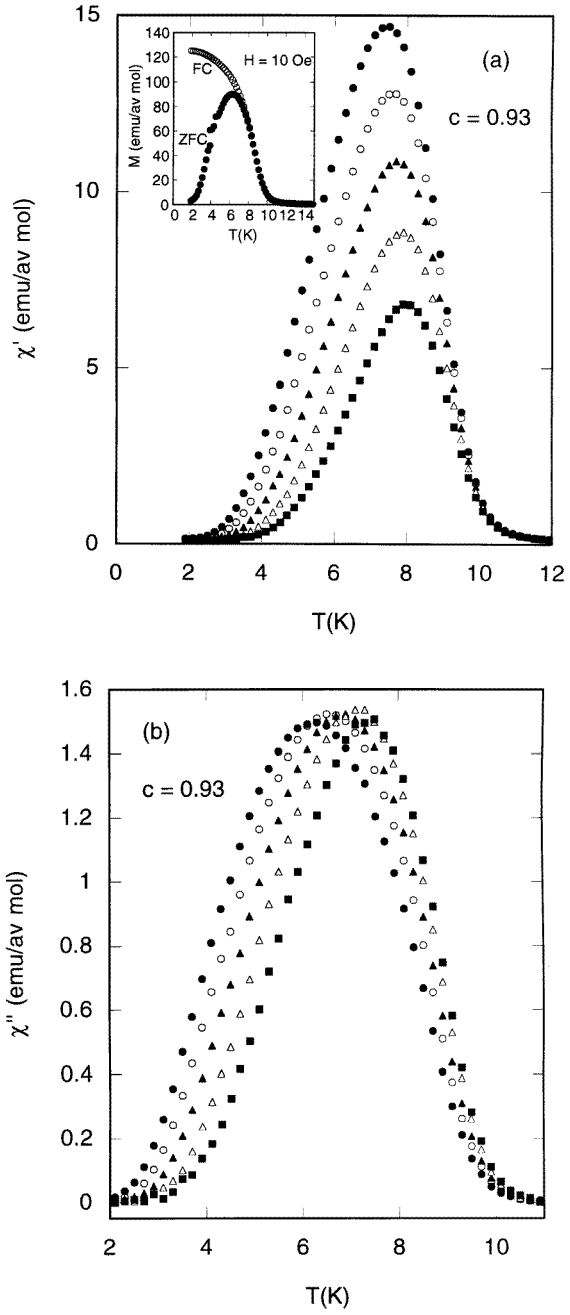

Figure 3. (a) χ' against T and (b) χ'' against T for $c = 0.93$ for various f. $f = 0.1$ (●), 1 (○), 10 (▲), 100 (△) and 1000 Hz (■). $H = 0$. $h = 50$ mOe. $h \perp c$. The T-dependence of M_{FC} (○) and M_{ZFC} (●) is shown in the inset of (a).

For $c = 0.93$ the peak of χ'' shifts to the lower temperature side with increasing H. The peak height drastically decreases with increasing H. The relationship between H and the peak temperature T_{SG} for χ'' is shown in the inset of figure 4(c). The least squares fit of the data to

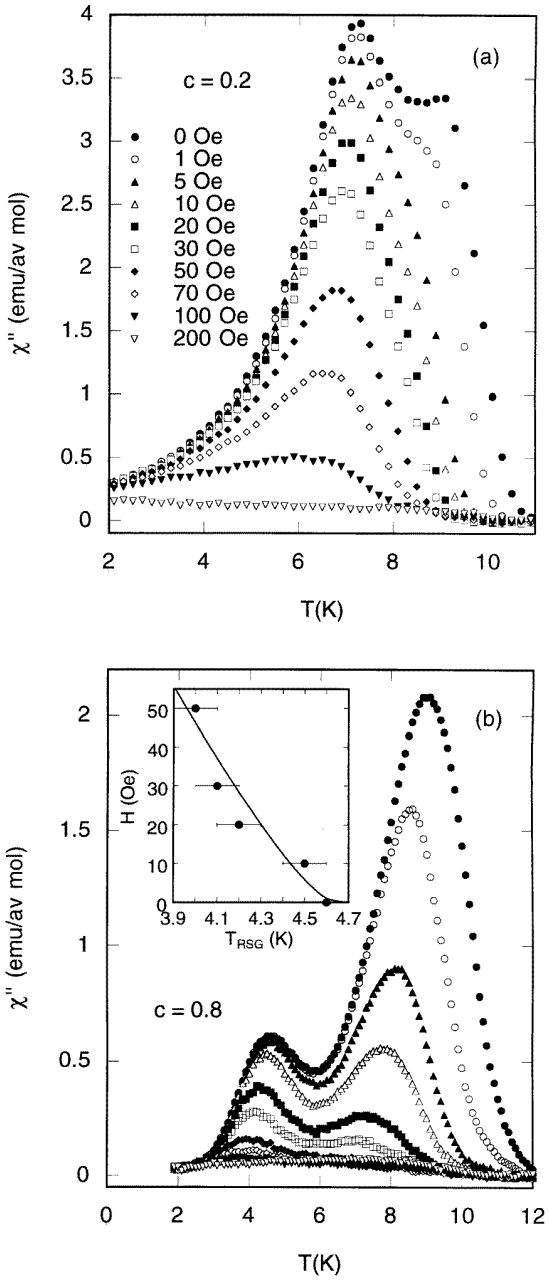

Figure 4. χ'' against T for various H. $H \perp c$. (a) $c = 0.2$, (b) $c = 0.8$ and (c) $c = 0.93$. $f = 100$ Hz. $h = 50$ mOe. $H = 0$ (●), 1 (○), 5 (▲), 10, (△), 20 (■), 30 (□), 50 (♦), 70 (◇), 100 (▼) and 200 Oe (▽). The plots of H against T_{RSG} and H against T_{SG} are shown in the insets of (b) and (c), respectively. The solid lines are the corresponding least squares fitting curves.

(1) yields the values with $H_0 = 988$ Oe, $T_{SG}(H = 0) = 7.28 \pm 0.20$ K and $a = 3.31 \pm 0.54$. This exponent a is much larger than that for the AT critical line, suggesting that the nature of the SG phase below T_{SG} is essentially different from that of the RSG phase below T_{RSG}.

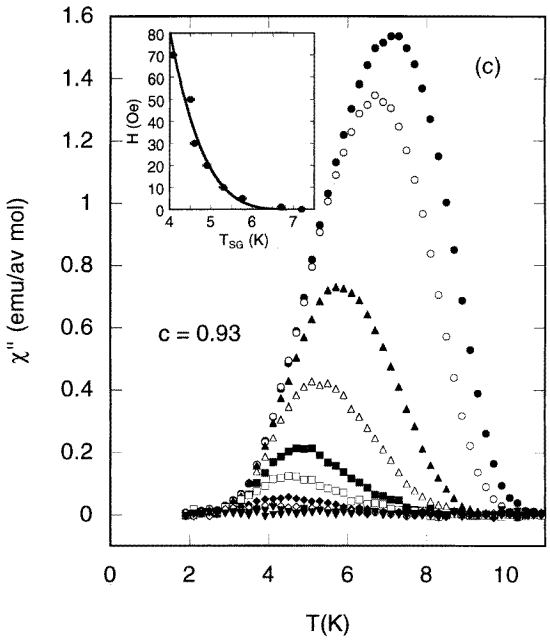

Figure 4. (Continued)

For $c = 0.5$ the peak temperature of χ'' decreases with increasing H: 4.3 K at $H = 0$ and 2.7 K at $H = 200$ Oe. This peak seems to disappear above this field. The least squares fit of the data of H against T_{RSG} to (1) yields $H_0 = 770$ Oe, $T_{RSG}(H = 0) = 4.04 \pm 0.08$ K and $a = 1.23 \pm 0.28$. The exponent a is almost the same as that for $c = 0.8$. The H-dependence of the AF (or FM) to RSG transition temperature has not been well examined theoretically. Experimentally it has been studied by Aruga *et al* [9] for $Fe_cMn_{1-c}TiO_3$ ($c = 0.65$) having the AF to RSG transition: as H increases $T_{RSG}(H)$ increases at low fields and in turn decreases above 7 kOe. In the higher field region $T_{RSG}(H)$ can be described by (1) with $a = 1.75$.

5. Discussion

5.1. Magnetic phase diagram

Figure 5 shows the critical temperature–Cu concentration phase diagram of stage-2 $Cu_cCo_{1-c}Cl_2$ GICs, where the critical temperatures are defined as peak temperatures of χ'' at $f = 0.1$ Hz. For $c = 0$ and 0.1 the phase transitions occur at T_{cu}, T_{p2} and T_{cl}. For $c = 0.2$ the phase transition at T_{p2} disappears. For $c = 0.3$ the peak of χ'' at T_{cu} becomes a shoulder, suggesting a weakly ordered phase below T_{cu}. The value of T_{cu} seems to be independent of Cu concentration for $0 \leqslant c \leqslant 0.3$. For $c = 0.4$ an RSG phase appears below T_{RSG}, in addition to a phase transition at T_c. For $0.5 \leqslant c \leqslant 0.9$ the value of T_{RSG} is almost independent of Cu concentration, while the value of T_c decreases with increasing Cu concentration. For $c = 0.93$ the phase transition at T_{RSG} disappears and the phase transition at T_c becomes spin-glass-like. For $c \approx 1$ no phase transition is observed at least above 0.3 K, partly because of the frustrated nature of the 2D antiferromagnet on the triangular lattice. Here we note that the critical temperature T_c for $0.4 \leqslant c \leqslant 0.93$ is considered to coincide with T_{cl} because T_c is lower than the peak temperature of χ' for each Cu concentration. Then the value of T_{cl} increases with

increasing Cu concentration and reaches a maximum around $c = 0.5$, where the probability P(Cu–Co) becomes a maximum. Such an enhancement of T_{cl} suggests that ferromagnetic interaction J(Cu–Co), which is comparable to or larger than J(Co–Co) above $c = 0.5$, plays an important role for the ferromagnetic long range order in each intercalate layer.

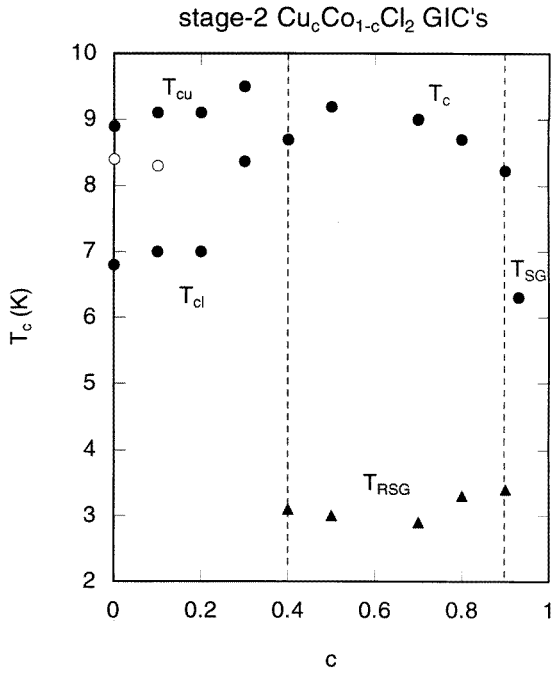

Figure 5. Magnetic phase diagram for stage-2 $Cu_cCo_{1-c}Cl_2$ GICs, where peak temperatures of χ'' at $f = 0.1$ Hz are plotted for each Cu concentration.

It is interesting to compare our magnetic phase diagram with those of other short-ranged random spin systems having competing interactions. For the 2D XY random spin systems $Rb_2Mn_cCr_{1-c}Cl_4$ on the square lattice, there exists a RSG phase for $0 < c \leqslant 0.5$ and an SG phase for $0.5 < c \leqslant 0.66$: a sequence of transitions from the PM to FM phase and from the FM to the RSG phase at a lower temperature for the RSG phase, and the transition from the PM to SG phase for the SG phase [10]. The temperature T_{RSG} is almost independent of Mn concentration. These results qualitatively agree well with those of stage-2 $Cu_cCo_{1-c}Cl_2$ GICs except for (i) the different critical concentrations for RSG and SG and (ii) the existence of an AF phase in $Rb_2Mn_cCr_{1-c}Cl_4$ with $c \approx 1$. The difference in critical concentrations is partly due to the different lattice symmetry and different nature of J(Cu–Co) and J(Mn–Cr). For $K_2Cu_cMn_{1-c}F_4$ (2D XY spin systems) on the square lattice sites, there is an SG phase for $0.5 < c \leqslant 0.8$. No RSG phase is observed [11].

5.2. Origin of RSG and SG phases

Here we discuss the origin of the RSG phase in our system. According to Aeppli *et al* [12] the RSG phase is caused by the random field effect. The ferromagnetic order is broken down by a random molecular field due to the freezing of spins in the PM clusters which do not contribute to the FM spin order. In the high temperature FM phase the fluctuations of the spins in the PM

clusters are so rapid that the FM network is less influenced by them and their effect is only to reduce the net FM moment. On approaching T_{RSG} the thermal fluctuations of the spins in the PM clusters become slower and the coupling between these spins and the FM network becomes significant. Then the molecular field from the slow PM spins acts as a random magnetic field, causing a break-up of the FM network into finite domains. This model is not appropriate to the RSG phase in our systems for the following reasons. It is known that the random field effect is realized in a random Ising antiferromagnet in the presence of H. In this case the long range spin order appears at low temperatures when the system is cooled in zero field, while no long range order is established when the system is cooled in the presence of H. This is not the case for our systems: M_{FC} is much larger than M_{ZFC}.

Kawamura and Tanemura [13, 14] have made a Monte Carlo study on the spin ordering process of the 2D $\pm J$ plane rotator (XY) model on the square lattice with the concentration of AF bonds c. For $c \approx 0$ the system undergoes a Kosterlitz–Thouless- (KT-) like transition at $T \approx J$. For $c = 0.5$ the system shows a novel type of SG transition into a chiral SG at $T \approx 0.3J$, which is characterized with the existence of frozen-in vortices. The nature of chiral SG is not sensitive to the concentration c. For $c < c_0$ (< 0.25) the reentrance phenomena are observed with the high temperature KT phase and the low temperature chiral SG phase. The uniform susceptibility of the FC state is larger than that of the ZFC state below T_{RSG}, indicating that the ZFC state of RSG phase is a metastable state. The frozen-in vortices produce such a domain structure. The domain size in the FC state is much larger than that in the ZFC state, because the magnetic field suppresses the generation of vortices.

The Cu concentration in our system does not coincide with the concentration of antiferromagnetic bonds in the above theory, because J(Cu–Co) is ferromagnetic. The lattice form of our system is different from that in the theory. The effect of interplanar interaction on the phase transition is not also taken into account in the theory. In spite of such differences, our result is qualitatively in good agreement with the prediction from the theory: (i) T_{RSG} is almost independent of Cu concentration, (ii) M_{FC} is much larger than M_{ZFC}, (iii) the magnetic phase diagram consists of the FM phase for $c \leqslant 0.3$, the high temperature FM phase and low temperature RSG phase for $0.4 \leqslant c \leqslant 0.9$ and an SG phase for $0.9 < c \leqslant 0.93$.

Here we note that Saslow and Parker [15] also have discussed the RSG transition in the 2D XY random spin system. They have shown that a sudden change in magnetization occurs at T_{RSG} in both of the heating and cooling conditions. This is not the case for M_{FC} in stage-2 $Cu_cCo_{1-c}Cl_2$ GICs which has no anomaly at T_{RSG}.

5.3. Exchange interaction $J(Cu–Co)$

The magnitude and sign of J(Cu–Co), which is crucial to the magnetic phase transitions of stage-2 $Cu_cCo_{1-c}Cl_2$ GICs, can be estimated from the data of Θ against c [1]. The Curie–Weiss temperature Θ monotonically decreases with increasing Cu concentration as listed in table 1. The sign of Θ changes from positive to negative for $0.8 \leqslant c \leqslant 0.85$, showing that the average intraplanar exchange interaction changes from ferromagnetic to antiferromagnetic. The value of Θ drastically decreases with increasing Cu concentration for $c > 0.95$. The Cu concentration dependence of Θ is predicted from the molecular field theory [1] as

$$\Theta = [c^2 P_{eff}^2(\mathrm{Cu})\Theta(\mathrm{Cu}) + (1-c)^2 P_{eff}^2(\mathrm{Co})\Theta(\mathrm{Co}) + 2\varepsilon c(1-c) \times \sqrt{|\Theta(\mathrm{Cu})\Theta(\mathrm{Co})|}\, P_{eff}(\mathrm{Cu})P_{eff}(\mathrm{Co})][cP_{eff}^2(\mathrm{Cu}) + (1-c)P_{eff}^2(\mathrm{Co})]^{-1} \quad (2)$$

where P_{eff}(Cu) ($= 2.26\ \mu_B$) and P_{eff}(Co) ($= 5.51\ \mu_B$) are the effective magnetic moments and Θ(Cu) $= -100.9$ K and Θ(Co) $= 23.2$ K are the Curie–Weiss temperatures of stage-2 $CuCl_2$ GIC and stage-2 $CoCl_2$ GIC, respectively. The intraplanar exchange interaction between

Cu^{2+} and Co^{2+} spins, J(Cu–Co), is defined as $J(\text{Cu–Co}) = \varepsilon[|J(\text{Cu–Cu})J(\text{Co–Co})|]^{1/2} = 16.14\varepsilon$ [K], where ε is a parameter to be determined. Here the interactions J(Co–Co) and J(Cu–Cu) are independent of concentration. The parameter ε can be calculated by substituting the value of Θ for each concentration into (2). The parameter ε is positive for any Cu concentration, and monotonically increases with increasing Cu concentration: $\varepsilon = 3.59c^3$ for intermediate concentration. This relation is not valid for low and high concentrations where the probability P(Cu–Co) becomes very small. These results suggest that J(Cu–Co) is larger than J(Co–Co) for $c > 0.51$ and is comparable to $|J(\text{Cu–Cu})|$ for $c \approx 0.83$ where the sign of Θ changes from positive to negative with increasing concentration. The concentration dependence of J(Cu–Co) may be related to the deformation of in-plane structure from an equilateral triangular lattice to an isosceles triangular lattice with increasing Cu concentration.

What is the origin of this ferromagnetic J(Cu–Co) interaction? The exchange interaction J(Cu–Co) between Cu^{2+} and Co^{2+} ions is a superexchange interaction through the Cl^- ions [16]. This superexchange interaction is considered to depend strongly on the distance between Cu^{2+} and Cl^-, the distance between Co^{2+} and Cl^- and angle between Cu–Cl and Co–Cl bonds. In the stage-2 $Cu_cCo_{1-c}Cl_2$ GICs the distance between Cu^{2+} ion and Cl^- ion, and the distance between Co^{2+} ion and Cl^- ion may change with concentration, but the angle between the Cu–Cl bond and Co–Cl bond is assumed to be independent of concentration and to be equal to $\phi = 90^\circ$. The ferromagnetic J(Cu–Co) may be explained in terms of the Goodenough–Kanamori rule for the $\phi = 90^\circ$ case where the Cu–Cl bond is perpendicular to the Co–Cl bond. The electron configurations of the lowest orbital states of Cu^{2+} and Co^{2+} which are subject to an octahedral field are given by $(\mathrm{d}\varepsilon^6)(\mathrm{d}\gamma^2)\,\mathrm{d}\gamma^1$ and $(\mathrm{d}\varepsilon^4)\,\mathrm{d}\varepsilon^1\,\mathrm{d}\gamma^2$, respectively, where those in parentheses indicate paired electrons. The Cl^- ion has two electrons with spins up and down. There is some probability that less than one electron is transferred from the p_σ orbital of Cl^- to the $\mathrm{d}\gamma$ orbital of Cu^{2+} because the p_σ orbital forms a partially covalent bond with the $\mathrm{d}\gamma$ orbital. The electron left behind on the Cl^- ion has its spin parallel to the spin of the Cu^{2+} ion. Since the p_σ orbital of the Cl^- ion is orthogonal to the $\mathrm{d}\gamma'$ orbital of the Co^{2+} ion, the direct exchange interaction between the remaining unpaired spin on the Cl^- ion and the Co^{2+} spins is ferromagnetic. This implies that the exchange interaction between Cu^{2+} and Co^{2+} spins is ferromagnetic.

5.4. Nature of RSG phase

The nature of RSG observed for $0.4 \leqslant c \leqslant 0.9$ is examined considering the f-dependence of χ'' for various T [17]. Figure 6 shows the f-dependence of χ' for $c = 0.8$ at various T values in the frequency range $0.007 \leqslant f \leqslant 1000$ Hz. It decreases with increasing f at any temperature between 1.9 and 11.7 K. The dispersion χ' can be well described by a power law form of ω ($\chi' \approx \omega^{-\zeta}$) over the whole frequency range studied for the following temperature ranges: $\zeta = 0.031$–0.035 at 1.9–2.0 K and 0.060–0.079 at 5.8–6.8 K. In the temperature range between 2.1 and 2.5 K χ' is fitted well to the power law form only in the low frequency range ($f \leqslant 0.1$ Hz). The value of ζ thus obtained decreases with decreasing T around 1.9–2.5 K.

The f-dependence of χ'' is much more complicated than that of χ'. Figure 7 shows the f-dependence of χ'' for $c = 0.8$ at various T values in the frequency range $0.007 \leqslant f \leqslant 1000$ Hz. As shown in figure 7(a) χ'' decreases with increasing f below 3.3 K. It has a local maximum, shifting to the higher frequency side with increasing T (0.07 Hz at 3.4 K and 330 Hz at 4.9 K), and a local minimum (0.03 Hz at 4.8 K and 360 Hz at 6.4 K). This shift of local maximum indicates that the lowest temperature phase is a RSG phase. The broad spectral width of up to 5.7 decades in frequency FWHM (full width at half maximum) (compared to a single time Debye fixed width of 1.14 decades) reflects an extremely broad distribution of relaxation times.

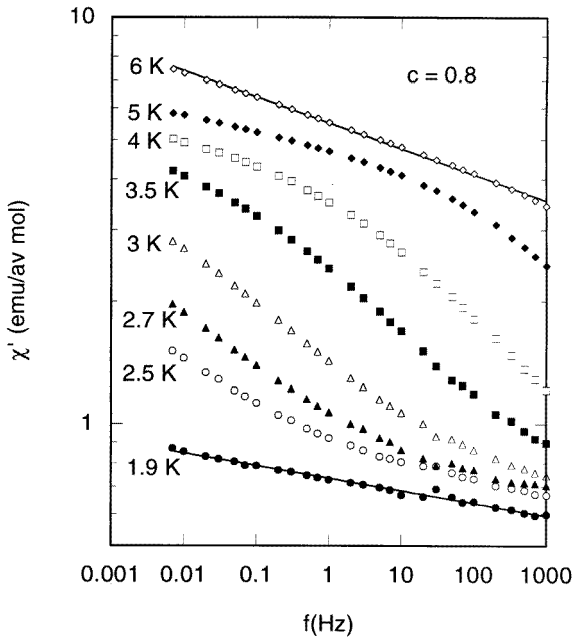

Figure 6. χ' against f for various T. $c = 0.8$. The solid lines are least squares fitting curves.

The maximum of χ'' against f provides a method for determining an average relaxation time τ for each T: $\omega\tau = 1$. The inset of figure 8 shows the average relaxation time τ as a function of T [7]. It divergingly increases with decreasing T. The most likely source for such a dramatic divergence of τ is a critical slowing down. We assume that $\chi''(\omega, T)$ is described by a scaling relation

$$\chi'' = A\omega^y f(\omega\tau) \tag{3}$$

where A is a constant, y is an exponent and $f(\omega\tau)$ is a scaling function of $\omega\tau$ having a peak at $\omega\tau = 1$. The relaxation time τ can be described by

$$\tau = \tau_0(T/T^* - 1)^{-x} \tag{4}$$

where $x = z\nu$, z is the dynamic critical exponent and ν is the exponent of the spin correlation length and T^* is a finite critical temperature. The least squares fit of the data of τ against T over the temperature range of 3.2–5.1 K yields the parameters $x = 13.8 \pm 1.4$, $T^* = 1.83 \pm 0.21$ K and $\tau_0 = 0.587 \pm 1.89$ s. The data of τ against T are also analysed for several models [17]. A fit of the Fulcher law, $\tau = \tau_0 \exp[E_0/k_B(T - T_0)]$ appears to yield fits of good quality. The activation energy E_0/k_B ($= 120 \pm 25$ K) is quite large and the characteristic temperature T_0 ($= -0.34 \pm 0.44$ K) is unphysical. Thus the Fulcher law may be ruled out. A fit of the droplet model, $\tau/\tau_0 \approx \exp[(b/T)^{1+x}]$ also appears to yield fits of good quality, where $\tau_0 = (0.3 \pm 2.1) \times 10^{-15}$ s and $b = 231 \pm 5$ K and $x = -0.16 \pm 0.19$. The negative x and large b are unphysical. So the drop model is also not appropriate.

It is predicted from (3) that χ'' can be described by a power-law ($\chi'' \approx \omega^y$) for $\omega\tau = 1$. The least squares fit of the data (peak value of χ'' against f) yields the exponent $y = 0.0089 \pm 0.0003$. In figure 8 we show the scaling plot of χ''/ω^y as a function of $\omega\tau$. We

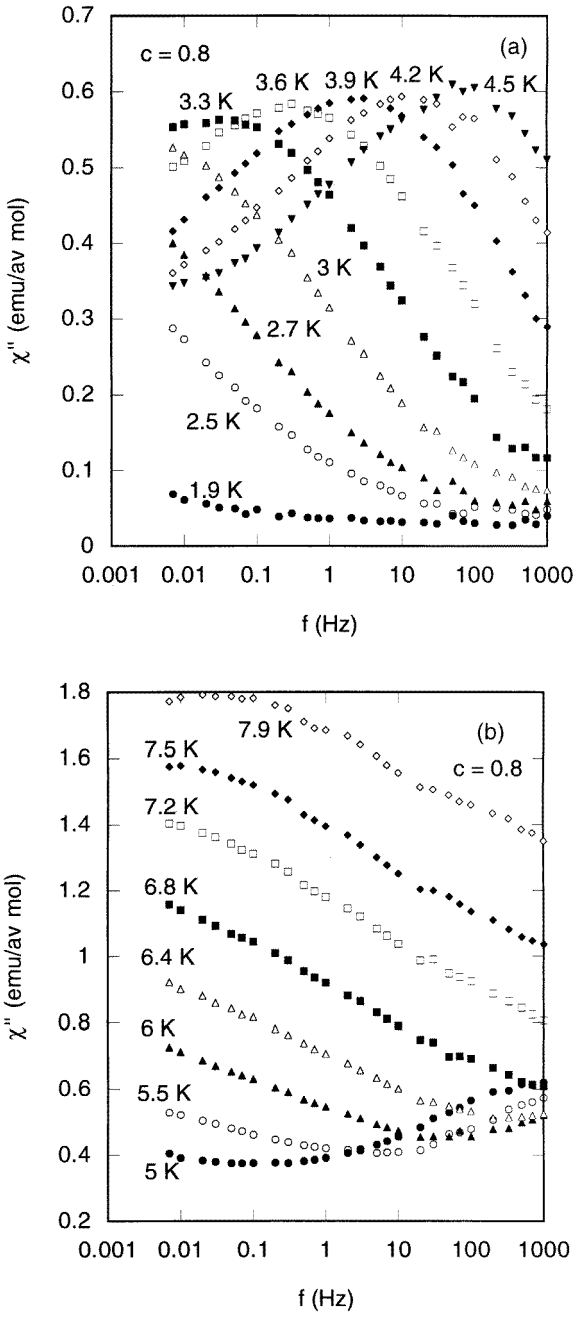

Figure 7. (a), (b), (c) and (d) χ'' against f for various T. $c = 0.8$.

find that almost all the data fall on a scaling function defined by

$$f(\omega\tau) = \mathrm{Im}\left[\frac{1}{1+(\mathrm{i}\omega\tau)^{1-\alpha}}\right] = \frac{\cos(\pi\alpha/2)/2}{\cosh[(1-\alpha)\ln(\omega\tau)] + \sin(\pi\alpha/2)} \qquad (5)$$

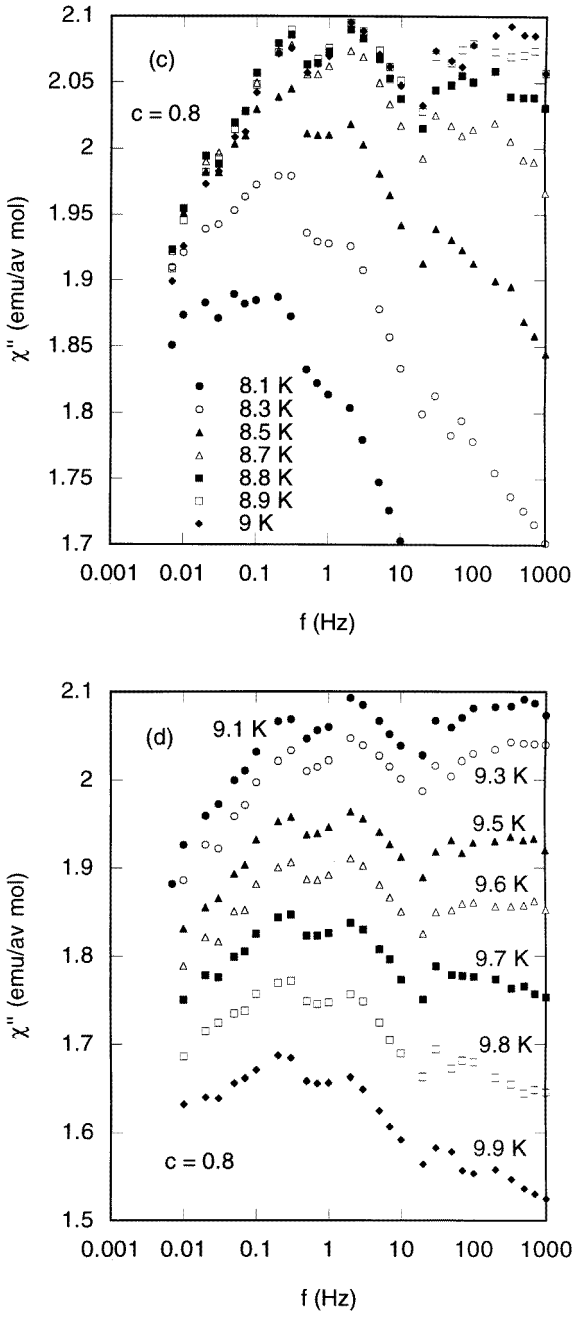

Figure 7. (Continued)

with $\alpha = 0.75 \pm 0.05$ for $0.01 \leqslant \omega\tau \leqslant 100$, where A in (3) is chosen as $A = 1.146\cos(\pi\alpha/2)/[1 + \sin(\pi\alpha/2)]$ so that χ''/ω^y takes 0.573 at $\omega\tau = 1$. The value of $\alpha = 0$ corresponds to the Debye equation for relaxation with a single time constant. The high value of α indicates that an extremely broad distribution of relaxation times persists throughout the whole temperature range studied.

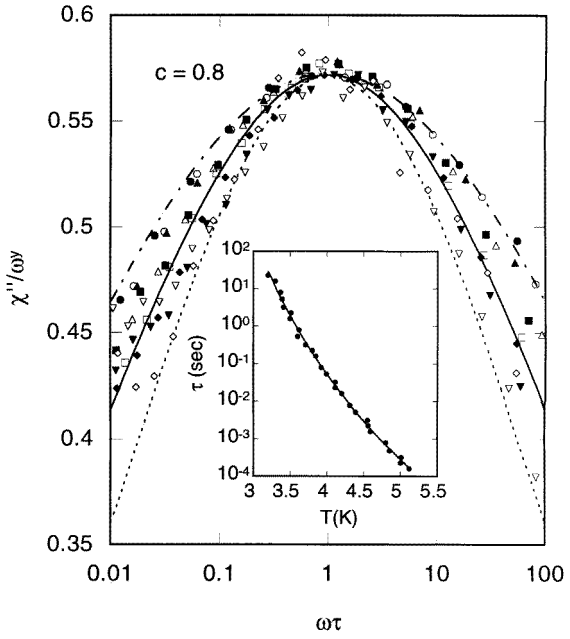

Figure 8. Plot of χ''/ω^y as a function of $\omega\tau$ for stage-2 $Cu_cCo_{1-c}Cl_2$ GIC with $c = 0.8$, where $y = 0.0089$ and $\tau = \tau_0(T/T^* - 1)^{-x}$ with $\tau_0 = 0.59$ s, $x = 13.81$ and $T^* = 1.825$ K: $f = 0.01$ (●), 0.05 (○), 0.1 (▲), 0.5 (△), 1 (■), 5 (□), 10 (♦), 50 (◇), 100 (▼) and 500 Hz (▽). The plot of τ against T is shown in the inset. The scaling function given by (5) is shown by a dotted line ($\alpha = 0.7$), solid line ($\alpha = 0.75$) and dash–dotted line ($\alpha = 0.80$), where a multiplicity constant is chosen so that the value of scaling function at $\omega\tau = 1$ coincides with the value of data.

The peak of χ'' around 3–4 K for $c = 0.5$, 0.7 and 0.88 also shifts to the low temperature side with decreasing f. This peak is also assumed to appear when the condition $\omega\tau = 1$ is satisfied. The T-dependence of τ is well fitted to (4) for the critical slowing down, in spite of the limited data, where $T^* = 1.78 \pm 0.79$ K and $x = 12.70 \pm 5.80$ for $c = 0.5$, $T^* = 1.28 \pm 0.12$ K and $x = 12.44 \pm 0.73$ for $c = 0.7$ and $T^* = 1.90 \pm 0.19$ K and $x = 8.51 \pm 1.20$ for $c = 0.88$. Monte Carlo simulation on a short range 3D Ising SG system has predicted $x = 7.9 \pm 1.0$ [18]. The value of x for $c = 0.88$ is close to this predicted value. The value of T^* is weakly dependent on Cu concentration: T^* is between 1.78 K and 1.90 K except for $c = 0.7$.

5.5. Nature of SG phase

The nature of the SG transition at $c = 0.93$ is examined from the f-dependence of χ'' for various T values. As shown in figure 3(b) the peak of χ'' shifts to the high temperature side with increasing f, indicating that the low temperature phase is an SG phase. The average relaxation time τ can be derived from the condition that the peak of χ'' occurs when $\omega\tau = 1$: τ decreases with increasing T. The data of τ against T are analysed for several models mentioned above. Although a fit of each model appears to yield fits of good quality partly because of the limited four data points, the parameters obtained for any model are unphysical: for example, $x = -0.35 \pm 1.00$ for the droplet model. Figure 9 shows the f-dependence of χ'' for $c = 0.93$ at various T in the frequency range $0.1 \leqslant f \leqslant 1000$ Hz. This f-dependence is rather different from that for $c = 0.8$. The absorption χ'' decreases with increasing f

below 5.9 K and increases with increasing f above 7.7 K. It shows a peak between 6.3 K and 7.5 K which shifts to the higher frequency side with increasing T. The f-dependence of χ'' at least in the temperature range between 5 and 8 K is described by (3) with $y = 0$ and $a \approx 0.87$. The broad spectral width of about eight decades in frequency reflects an extremely broad distribution of relaxation times.

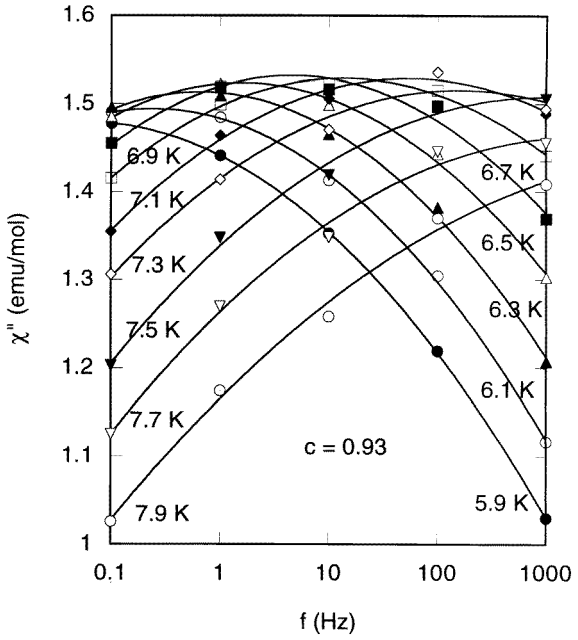

Figure 9. χ'' against f for various T. $c = 0.93$. The solid lines are smoothing curves for data.

5.6. Nature of FM phases at $c = 0$ and 0.8

The nature of the FM phase for $0 \leqslant c \leqslant 0.3$ and $0.4 \leqslant c \leqslant 0.9$ is examined considering the f-dependence of χ'' for $c = 0$ and 0.8, respectively. The f-dependence of χ'' at $c = 0$ has the following features [5]. For $1.9 \leqslant T \leqslant 6.2$ K χ'' decreases slightly with increasing f. At 6.3 K χ'' is almost independent of f except for a local minimum around $f = 10$ Hz. Between 6.7 K just below T_{cl} (= 6.9–7.1 K) and T_{cu} (= 8.9 K), χ'' shows two small peaks at $f = 0.2$–0.3 and 2–3 Hz and it increases with increasing f for $f \geqslant 20$ Hz. Around 9.5 K χ'' becomes almost independent of f and it tends to decrease slightly with increasing f for $9.7 \leqslant T \leqslant 10.7$ K.

We have shown that these phenomena can be explained in terms of the following model [5]. Between T_{cu} and T_{cl} the interisland correlation is still random within each intercalate layer. The magnetization of each island fluctuates and changes direction relative to other islands in a certain characteristic time scale depending on the island size and interisland interaction. The relaxation time τ_{out} related to the interisland fluctuations is much larger than τ_{in} related to the intraisland fluctuations. Correspondingly the characteristic frequency f_{in} defined by $(2\pi\tau_{in})^{-1}$ is much larger than f_{out} defined as $(2\pi\tau_{out})^{-1}$. When the relaxation of these fluctuations is of Debye type, the absorption χ'' may be described by [5]

$$\chi''(\omega) = \chi^{in}(\boldsymbol{Q} = \boldsymbol{0})\frac{\omega\tau_{in}}{1 + (\omega\tau_{in})^2} + \chi^{out}(\boldsymbol{Q} = \boldsymbol{0})\frac{\omega\tau_{out}}{1 + (\omega\tau_{out})^2}. \tag{6}$$

Here $\chi^{in}(\boldsymbol{Q})$ and $\chi^{out}(\boldsymbol{Q})$ are the wavevector dependent susceptibilities related to the intraisland and interisland fluctuations, respectively. The static susceptibilities $\chi^{in}(\boldsymbol{Q}=\boldsymbol{0})$ and $\chi^{out}(\boldsymbol{Q}=\boldsymbol{0})$ may diverge at T_{cu} and T_{cl}, respectively. The absorption χ'' exhibits maxima at $\omega\tau_{in}=1$ and $\omega\tau_{out}=1$ depending on temperature.

For $c=0$ the decrease of χ'' with increasing f below T_{cl} is due to the relaxation of interisland fluctuations with $f_{out}<0.1$ Hz. The drastic increase of χ'' for $f\geqslant 20$ Hz between T_{cl} and T_{cu} is due to the relaxation of intraisland fluctuations with $f_{out}>1$ kHz. The peak of χ'' at $f=0.2$–0.3 and 2–3 Hz between T_{cl} and T_{cu} is due to the relaxation of interisland fluctuations with $f_{out}=0.2$–0.3 and 2–3 Hz.

The f-dependence of χ'' for $c=0.8$ above 5 K is shown in figures 7(b)–(d). The increase of χ'' with increasing f near 1 kHz for $5\leqslant T\leqslant 6.3$ K (see figure 7(b)) is due to the relaxation of fluctuations associated with the RSG phase. The corresponding characteristic frequency for the RSG phase, which increases with increasing T, is larger than 1 kHz above 5 K. Between 6.4 and 7.5 K χ'' decreases with increasing f for $0.007\leqslant f\leqslant 1000$ Hz. Note that χ'' for $6.5\leqslant T\leqslant 7.5$ K is well described by a power law form ($\chi''\approx\omega^{-y}$) for $0.007\text{ Hz}\leqslant f\leqslant 1$ kHz: $y=0.052\pm 0.001$ at 7 K and $y=0.038\pm 0.001$ at 7.5 K.

At 7.7 K χ'' has a broad peak at $f=0.02$ Hz. The absorption χ'' is described by a form similar to (5) with a characteristic relaxation time τ ($=1/2\pi f$) and the parameter α close to 0.85, indicating an extremely broad distribution of relaxation times in this system. This peak shifts to the high frequency side with increasing T: $f=0.2$–0.3 Hz for $8.2\leqslant T\leqslant 10$ K. In addition to this peak, at least three broad peaks newly appear at $f=2-3$ Hz for $8.5\leqslant T\leqslant 10$ K, 20–30 Hz for $8.2\leqslant T\leqslant 8.7$ K and 300 Hz for $8.7\leqslant T\leqslant 9.4$ K, respectively (see figures 7(c) and (d)). Note that $T_{cl}=8.7$ K is identified as the peak temperature of χ'' at $f=0.01$ Hz for $c=0.8$. The appearance of such peaks reflects the complex nature of spin orderings in this system. Two low frequencies ($f=0.2$–0.3 and 2–3 Hz) coincide with the value of f_{out} for $c=0$, while the high frequency ($f=300$ Hz) may correspond to f_{in} (>1 kHz) for $c=0$. The relatively weak peak of χ'' at $f=300$ Hz is indicative of weak divergence in $\chi^{in}(\boldsymbol{Q}=\boldsymbol{0})$ because of the spin frustration effect occurring inside each island. This peak height of χ'' at $f=300$ Hz has a maximum around 9 K which may correspond to T_{cu}. In spite of the difference in the detail of the f-dependence of χ'', it may be concluded that the nature of the FM phase for $c=0.8$ is essentially the same as that for $c=0$.

6. Conclusion

We have shown that stage-2 $Cu_cCo_{1-c}Cl_2$ GICs magnetically behave like a 2D XY spin glass on the triangular lattice, where the ferromagnetic intraplanar exchange interactions J(Cu–Co) and J(Co–Co) compete with the AF intraplanar exchange interaction J(Cu–Cu). The FM phase for $0.4\leqslant c\leqslant 0.9$ is essentially the same as that for $0\leqslant c\leqslant 0.3$. The RSG and SG phases appear for $0.4\leqslant c\leqslant 0.9$ and $c=0.93$, respectively. The dynamic critical behaviour of the RSG phase is of the conventional type with critical slowing down. The RSG phase may be related to a chiral SG characterized by the existence of frozen-in vortices. The SG phase arising from the competition between J(Cu–Co) and J(Cu–Cu) is characterized by an extremely broad distribution of relaxation times. No phase transition is observed near $c\approx 1$ because of the fully frustrated nature of the antiferromagnet on the triangular lattice. Magnetic neutron scattering studies are required for further understanding of RSG, SG and FM phases.

Acknowledgments

We would like to thank A W Moore and H Suematsu for providing us with HOPG and SCKG, respectively. We are grateful to M D Johnson, J Morillo, T Shima, B Olson and K de Vries for their help in sample preparation and C R Burr for a critical reading of this manuscript. This work was partly supported by NSF grants DMR-9201656 and 9625829.

References

[1] Suzuki M, Suzuki I S, Johnson M D, Morillo J and Burr C R 1994 *Phys. Rev.* B **50** 205–15
[2] Suzuki M, Suzuki I S, Burr C R, Wiesler D G, Rosov N and Koga K 1994 *Phys. Rev.* B **50** 9188–99
[3] Dresselhaus G, Nicholls J T and Dresselhaus M S 1992 *Graphite Intercalation Compounds II* ed H Zabel and S A Solin (Berlin: Springer) pp 247–345
[4] Suzuki M 1990 *Crit. Rev. Solid State Mater. Sci.* **16** 237–54
[5] Suzuki M and Suzuki I S 1998 *Phys. Rev.* B **58** 840–6
[6] Wiesler D G, Suzuki M and Zabel H 1987 *Phys. Rev.* B **36** 7051–62
Wiesler D G and Zabel H 1987 *Phys. Rev.* B **36** 7303–6
Wiesler D G, Zabel H and Shapiro S M 1994 *Z. Phys.* B **93** 277–97
[7] Suzuki I S and Suzuki M 1998 *Solid State Commun.* **106** 513–17
[8] de Almeida J R L and Thouless D J 1978 *J. Phys. A: Math. Gen.* **11** 983–90
[9] Aruga H, Ito A, Wakabayashi H and Goto T 1988 *J. Phys. Soc. Japan* **57** 2636–9
[10] Katsumata K, Tuchendler J, Uemura Y J and Yoshizawa H 1988 *Phys. Rev.* B **37** 356–69
[11] Kimishima Y, Ikeda H, Furukawa A and Nagano H 1986 *J. Phys. Soc. Japan* **55** 3574–84
[12] Aeppli G, Shapiro S M, Birgeneau R J and Chen H S 1983 *Phys. Rev.* B **28** 5160–72
[13] Kawamura H and Tanemura M 1985 *J. Phys. Soc. Japan* **54** 4479–82
[14] Kawamura H and Tanemura M 1986 *J. Phys. Soc. Japan* **55** 1802–5
[15] Saslow W M and Parker G 1986 *Phys. Rev. Lett.* **56** 1074–7
[16] Kanamori J 1959 *J. Phys. Chem. Solids* **10** 87–98
[17] Mydosh J A 1993 *Spin Glasses: an Experimental Introduction* (Washington, DC: Taylor and Francis). See also references therein for theoretical models
[18] Ogielski A T 1985 *Phys. Rev.* B **32** 7384–98